Numerical modelling of thin-walled Z-columns made of general laminates subjected to uniform shortening

Andrzej Teter[1]* and Zbigniew Kołakowski[2]

[1] *Faculty of Mechanical Engineering, Department of Applied Mechanics, Lublin University of Technology*
Nadbystrzycka 36, 20-618 Lublin, Poland
e-mail: a.teter@pollub.pl

[2] *Department of Strength of Materials (K12), Lodz University of Technology*
Stefanowskiego 1/15, 90-924 Lodz,, Poland
e-mail: zbigniew.kolakowski@p.lodz.pl

Abstract

The numerical modelling of a plate structure was performed by the finite element method and one-mode approach based on Koiter's method. The first order approximation of Koiter's method enables to solve the eigenvalue problem. The second order approximation describes post-buckling equilibrium paths. In the finite element analysis, the Lanczos method was used to solve the linear problem of buckling. The simulations of the non-linear problem were performed using the Newton–Raphson method. The numerical results were then verified in experimental tests using the strain-gauge technique. Detailed calculations were made for short Z-columns made of general laminates. The static compression test was performed. The specimens were simply supported on both ends.

Keywords: Koiter's method, FEM, general laminate, compression test, coupling effect, classical lamination theory, FRP

1. Introduction

A general laminate has many layers and the arrangement of layers is non-symmetric. The main disadvantage of a general laminate is that mechanical coupling effects occur. Different types of coupling between extension/compression, shearing, bending and twisting can take place [4-5]. According to the classical laminate theory [2], the constitutive equation can be written as:

$$\begin{Bmatrix} \{N\} \\ \{M\} \end{Bmatrix} = [K] \begin{Bmatrix} \{\varepsilon^o\} \\ \{\kappa\} \end{Bmatrix} \quad \text{and} \quad [K] = \begin{bmatrix} [A] & [B] \\ [B] & [D] \end{bmatrix} \tag{1}$$

The stiffness matrix $[K]$ defines the relationship between section forces/moments and deformation/curvature. The K-matrix can be divided into three submatrices: extensional (i.e., $[A]$), coupling (i.e., $[B]$) and bending (i.e., $[D]$). The elements of the A-submatrix denoted as A_{16} and A_{26} describe the in-plane coupling effects. In this case, an interaction between shearing and extension or compression occurs. In contrast, the elements of the D-submatrix denoted as D_{16} and D_{26} describe the out-plane coupling effects. Here, one can observe an interaction between bending and twisting.

2. Numerical modelling

Thin-walled structures can exhibit many different buckling modes depending on their length. If a structure is short, local buckling takes place. It is the first buckling mode, and the corresponding buckling stresses are the lowest. With longer columns, coupling buckling may occur if two or more eigenvalue loads are nearly identical. Finally, one can distinguish global buckling which is typical of long structures.

The numerical modelling of the buckling behaviour of plate structures can be performed using the analytical–numerical method (ANM) [3] based on Koiter's asymptotic method (Fig. 1a) or finite element method (FEM) (Fig. 1b). Both methods allow us to determine the static and dynamic buckling stresses as well as the post-buckling equilibrium path of a plate structure subjected to various types of loads. The numerical results should then be verified in experimental tests performed on real structures (Fig. 1c).

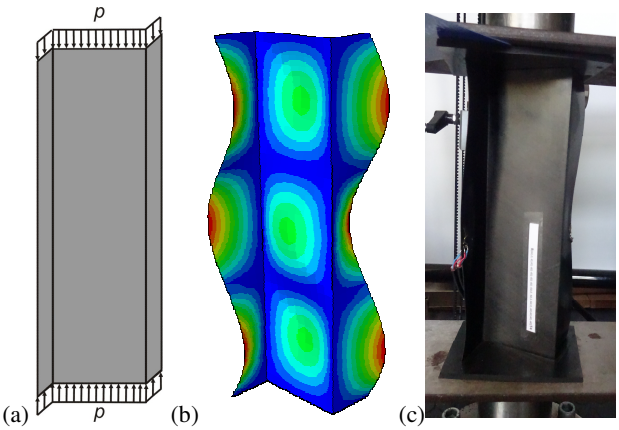

Figure 1: Modelling of Z-column buckling: (a) ANM model; (b) FEM model; (c) experimental model

2.1. *One-mode approach based on Koiter's method (ANM)*

In the analytical–numerical method [3], a plate model was used for all walls of the structure (Fig. 1a). Using variational principles, the differential equations of equilibrium can be obtained. The solution of these equations should satisfy the initial conditions, the kinematic and static continuity conditions at the junctions of adjacent plates, and the boundary conditions. If the number of interacting buckling modes is 1, the solution is

* ACKNOWLEDGEMENTS: This paper was financially supported by the Ministerial Research Project No. DEC-2013/11/B/ST8/04358 financed by the Polish National Science Centre.

a one-mode approach (i.e., uncoupled buckling). In this case, the differential equation of equilibrium can be written as [3]:

$$\left(1 - P/P_{cr}\right)\xi + b_{111}\,\xi^2 + c_{1111}\,\xi^3 = \xi^* P/P_{cr} \qquad (2)$$

where: $\zeta = w/t$ is the dimensionless amplitude of the buckling mode (w - maximum deflection, t - thickness), P_{cr}, P, $\zeta^* = w/t$ are the buckling loads, compression loads and dimensionless amplitude of the initial deflection corresponding to the buckling mode (w_o – maximum initial deflection), respectively, b_{111} is the coefficient in the first order approximation, c_{1111} is the coefficient in the second approximation.

2.2. *Finite element method (FEM)*

The numerical simulations were performed with the Abaqus system [1]. The FE-model of the analysed column (Fig. 1b) was composed of multi-layered shell elements with 8 nodes. The elements had six degrees of freedom at each node. The FEM analysis involved solving the eigenvalue problem of buckling using the Lanczos method. Next, post-buckling paths were determined by a nonlinear buckling analysis. The Newton–Raphson method was employed.

2.3. *Experimental verification*

The experimental studies were conducted using a universal testing machine and a special grip made of two identical parts. One part consisted of a rigid steel plate and a clamping sleeve. The speed of the upper cross beam in the testing machine was maintained constant at 1 mm/min. The compressive load and strains in the direction of load were measured. The strain gauges were located on the opposite sides of the column wall in the region of the highest half-wave amplitude determined by FE analysis (Fig. 1a).

3. Results

All tests were performed on Z-columns under uniform shortening. The dimensions of their cross-section are shown in Fig. 2. The specimens were simply supported on both ends.

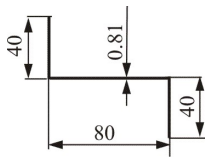

Figure 2: Dimensions of the cross-section in mm

The stacking sequences of the laminate were: $[60,0,-60,60,-60_5,(0,-60)_3,60_2,-60]_T$ (i.e., Case 1), $[60,0,-60_2,60_5,(0,60)_2,0,-60_2,60_2]_T$ (i.e., Case 2), $[60,0_2,-60_2,60_3,-60_2,0_3,-60_2,0,60_2]_T$ (i.e., Case 3), respectively. The lengths of the specimens were: 270mm (Cases 1 and 2) and 330mm (Case 3). The amplitude of imperfection related to the first buckling mode was equal to 1/10 of the column wall thickness. The mechanical properties of the carbon-epoxy laminate were as follows: Young's modulus in fibre direction (i.e., direction 1) was 170 GPa and in transverse direction of the fibers (i.e., direction 2) – 7.6 GPa, respectively; Poisson's ratio in plane 1-2 was 0.36; shear modulus in plane 1-2 was 3.52 GPa.

The first step involved determining buckling loads. A numerical analysis was performed to solve the eigenvalue problem. The experimental buckling loads were determined by the following methods: vertical tangent method (P1), averaged strain method (P2), P-w method (P3), P-w^2 method (P4), inflection point method (P5) and Koiter's method (P6). Since the effect of bifurcation does not occur in the experimental tests, it was possible to determine the approximate buckling load. Details are given in Table 1. The second step consisted in performing a post-buckling analysis. In Fig. 3, the numerical solutions are compared in dimensionless form.

Table 1: Buckling loads in N

No	FEM			ANM			Test		
	Case1	Case2	Case3	Case1	Case2	Case3	Case1	Case2	Case3
P1	1913	1856	1744	1941	1831	1639	1749	1675	1292
P2							1673	1600.	1252
P3							1660	1695	1257
P4							1690	1567	1277
P5							1850	1819	1505
P6							1654	1503	1207

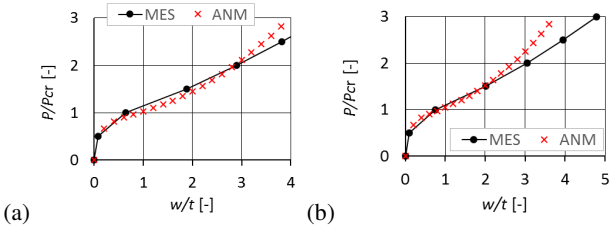

Figure 3: Post-buckling paths: (a) Cases 1 and 2, (b) Case 3

4. Conclusions

The application of the ANM method provides very effective solutions for all types of thin-walled structures subjected to various types of loads. All static and dynamic buckling analyses of thin-walled structures can be conducted with this method. Moreover, in contrast to the FEM, the ANM calculations can be done much faster and easier, and the results show a satisfactory accuracy. Nonetheless, the visualization of results is much easier in the FEM. Given that the results obtained with the two methods and the experimental findings were similar, it can be concluded that the proposed modelling technique yields accurate results. The study has revealed that it is only the twisting-bending coupling effect that has a significant impact on the buckling behaviour of the compressed structures.

References

[1] Debski H., Teter A. and Kubiak T., Numerical and experimental studies of compressed composite columns with complex open cross-sections, *Composite Structures* 118, pp. 28–36, 2014.

[2] Jones RM. *Mechanics of Composite Materials*, 2nd ed. Taylor & Francis, London, 1999.

[3] Kołakowski Z. and Teter A., Coupled static and dynamic buckling modelling of thin-walled structures in elastic range review of selected problems, *Acta Mechanica et Automatica*, 10(2), pp. 141-149, 2016.

[4] Teter A. and Kolakowski Z., Influence of mechanical couplings on the buckling behaviour of thin-walled plates made of general laminates under compression, *Composite Structures* 166, pp. 68–76, 2017.

[5] York C.B., Tapered hygro-thermally curvature-stable laminates with non-standard ply orientations, *Composites: Part A*, 44, pp. 140–148, 2013.